Inorganic Chemistry

Article

pubs.acs.org/IC

Pressure-Induced Structures and Properties in Indium Hydrides

Yunxian Liu,[†] Defang Duan,[†] Fubo Tian,[†] Hanyu Liu,[‡] Chao Wang,[†] Xiaoli Huang,[†] Da Li,[†] Yanbin Ma,[†] Bingbing Liu,[†] and Tian Cui*[,†]

[†]State Key Laboratory of Superhard Materials, College of Physics, Jilin University, Changchun, 130012, People's Republic of China

[‡]Geophysical Laboratory, Carnegie Institution of Washington, Washington D.C. 20015, United States

Supporting Information

ABSTRACT: The structures, electron properties, and potential superconductivity of indium hydrides are systematically studied under high pressure by first-principles density functional calculations. Upon compression, two stable stoichiometries (InH_3 and InH_5) are predicted to be thermodynamically stable. Particularly, in the two compounds, all hydrogen atoms exist in the form of H_2 or H_3 units. The stable phases present metallic features with the overlap between the conduction and the valence bands. The Bader analysis indicates that charges transfer from In atoms to H atoms. Electron−phonon calculations show that the estimated transition temperatures (T_c) of InH_3 and InH_5 are 34.1−40.5 and 22.4−27.1 K at 200 and 150 GPa, respectively.

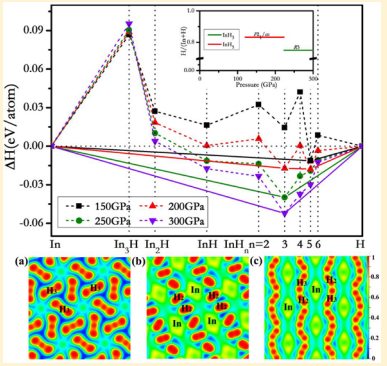

INTRODUCTION

It was reported that hydrogen may become a high-temperature superconductor.[1] So searching for metallic hydrogen has been the focus of our research. When the pressure is increased up to 360 GPa in experiments, however, hydrogen continues to remain insulating.[2] Thus, interest has increased in hydrogen-rich compounds, due to the fact that they have the potential to become metallic and extraordinary superconductors ("chemical precompression") at lower pressures than pure hydrogen. The crystal structural features and superconductivities of some hydrogen-rich compounds have been extensively explored under high pressure. Meanwhile, it is well established that pressure can be employed to affect some properties of substance and induce the formation of new materials. For example, because the metalization of SiH_4 can occur at relatively lower pressures, theoretical and experimental research has made considerable progress toward exploring its structures and superconductivity.[3−9] Certain hydrides have also been predicted to have high superconductivities with T_c reaching 17.7 K at 40 GPa for YH_3,[10] 58.6−69.8 K at 166 GPa for KH_6,[11] 191−204 K at 200 GPa for H_3S,[12] 41.2−47.2 K at 200 GPa for PoH_4,[13] 106 K at 150 GPa for SbH_4[14] and so on. Some hydrides with large hydrogen fractions were also formed under high pressure (e.g., Na−H, K−H, Rb−H, Cs−H, Sc−H, Y−H, Os−H).[11,15−20] The investigation of the above hydrides has reignited great interest in studying other H-rich compounds.

Group IIIA includes boron (B), aluminum (Al), gallium (Ga), indium (In), and thallium (Tl) elements. Hydrides of B, Al, and Ga have been extensively researched in theory and experiment and show outstanding properties under pressure.[21−23] For instance, a theoretical work indicated that, in the B−H system, BH and B_2H_6 can coexist in a wide pressure range, and BH is a superconductor with a T_c of 14.1−21.4 K at 175 GPa.[21] AlH_3 can be used as a hydrogen storage material with a relatively high hydrogen gravimetric density of 10.1 wt %.[22] The high-pressure structure (Pm-3n) of GaH_3 was predicted to be a superconductor with a high T_c (73−86 K at 160 GPa).[23] InH_3 is thermodynamically unstable in both the gas phase and the solid state under normal conditions.[24] To our best knowledge, pressure can be applied to produce novel hydrides that cannot be formed at ambient conditions, and the investigation of indium hydrides under pressure is not well explored yet. Therefore, we became interested in indium hydrides, as we are curious about what structures and properties they would show, in particular the existent form of H and superconductivity of indium hydrides and which stoichiometric indium hydrides are thermodynamically stable at a given pressure. Herein, we carry out a systematic investigation on the hitherto unknown indium hydrides at high pressures, as well as their properties.

In this article, we extensively search various stoichiometries of indium hydrides at zero temperature by the first-principles global structural optimization method. In addition, the high-pressure stability of different stoichiometries as a function of pressure, dynamical stabilities, electronic properties, and superconductive behaviors of the optimum static structures is systematically investigated. Above 150 GPa, two metallic H-rich stoichiometries, InH_3 and InH_5, become stable. Moreover, InH_3 and InH_5 adopt structures with H_3 and H_2 units, respectively. With the help of the electron localization functions, we find that there exists strong polar covalent bonding in H_2 or H_3 units,

Received: July 27, 2015
Published: October 2, 2015

DOI: 10.1021/acs.inorgchem.5b01684
Inorg. Chem. 2015, 54, 9924−9928

and the Bader charge analysis shows that the charges transfer from In to H atoms. To study the superconductivity of InH_3 and InH_5, we calculated the superconducting critical temperature (T_c) values by the Allen−Dynes-modified McMillan equation, which shows high T_c values of 34.1−40.5 K for InH_3-R-3 and 22.4−27.1 K for InH_5-$P2_1/m$ at 200 and 150 GPa, respectively.

COMPUTATIONAL METHOD

The ground-stable structure predictions of In_3H, In_2H, and InH_n (n = 1−6) were carried out via the evolutionary algorithm USPEX, as implemented in the USPEX code (universal structure predictor: Evolutionary Xtallography).[25−27] Evolutionary simulations were implemented at 50, 100, 200, and 300 GPa with system sizes of 1, 2, 3, and 4 formula units per cell, all at 0 K. We performed the structural relaxations and electronic structure calculations with the Perdew−Burke−Ernzerh (PBE) parametrizations of the generalized gradient approximation (GGA),[28] as implemented in the Vienna Ab-Initio Simulation Package (VASP) code,[29] which is based on the density functional theory. The all-electron projector-augmented wave method (PAW)[30] was adopted for In and H with an electronic configuration of $5s^25p^1$ and 1s, respectively. We took 0.8 au and 3.1 au for the cutoff radius of H and In, respectively. A tested energy cutoff of 800 eV and appropriate Monkhorst−Pack Brillouin sampling grid of spacing $2\pi \times 0.03$ Å^{-1} were used for all cases, ensuring a total energy convergence of less than 1 meV. The phonon calculations were performed by using a supercell approach[31] through the PHONOPY code.[32] The Bader charge analysis[33−35] was employed to perform charge calculations. The superconductivities of stable phases were performed within the framework of the linear-response theory via the Quantum-ESPRESSO package.[36] The superconducting critical temperature T_c was estimated by using the Allen−Dynes-modified McMillan equation[37] $T_c = (\omega_{log}/1.2)\exp[1.04(1+\lambda)/\lambda - \mu^*(1+0.62\lambda)]$. The parameters ω_{log}, λ, and μ^* denote the logarithmic average frequency, the electron−phonon spectra, and the Coulomb pseudopotential, respectively. Convergence tests provided a suitable value of 80 Ry for the kinetic energy cutoff, and norm-conserving pseudopotentials were adopted. In the first Brillouin zone, the q-point meshes of 3 × 3 × 3 and 3 × 4 × 2 were used for R-3 (InH_3) and $P2_1/m$ (InH_5) structures, respectively.

RESULTS AND DISCUSSION

In this work, stable stoichiometries and structures for In_3H, In_2H, and InH_n (n = 1−6) were investigated over the pressure range of 50−300 GPa. Figure 1 shows the formation enthalpies of the most favorable structures for each composition relative to elemental indium and hydrogen at given pressures. In addition, the enthalpies of $I4/mmm$ and $Fmmm$ for In (which are based on our evolutionary searches) and $P6_3/m$, $C2/c$, and $Cmca$ for H_2[38] were selected as the reference of thermodynamics. The convex hull was formed by thermodynamically stable or metastable compositions, which can be synthesized experimentally in principle. As seen in Figure 1, at 150 GPa, InH_5 is the first stable composition with the most negative enthalpy of formation. When the pressure is increased up to 200 GPa, both InH_5 and InH_3 emerge on the convex hull, and InH_5 is still the global minimum compound. With increasing pressure, InH_3 is the only stable stoichiometric hydride at 200−300 GPa. Meanwhile, the inset map (in Figure 1) gives the stable pressure ranges of InH_3 and InH_5. We can see that the phase $P2_1/m$ of InH_5 is stable in the pressure range from 120 to 223 GPa. It is suggested that InH_5 might be synthesized via the reaction $2In + 5H_2 \rightarrow 2InH_5$ above 120 GPa, and it remains stable up to 223 GPa. Then InH_5 decomposes into InH_3 ($R\bar{3}$) and H_2 above 233 GPa via the reaction $InH_5 \rightarrow InH_3 + H_2$, and InH_3 remains favorable up to 300 GPa.

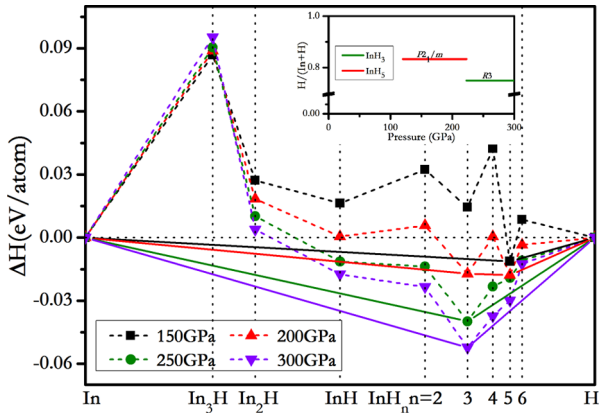

Figure 1. Calculated formation enthalpies (ΔH in eV per atom) of In_3H, In_2H, and InH_n (n = 1−6) with respect to In and H at different pressures. Inset: The stable pressure ranges of InH_3 and InH_5.

The motifs of crystal structures for two stable compounds (InH_5 and InH_3) are depicted in Figure 2. InH_5 was predicted to possess a monoclinic $P2_1/m$ structure and a triclinic P-1 phase at 200 and 300 GPa, respectively. Notice that, in the $P2_1/m$ phase, the In atoms are in the form of a one-dimensional chain and H_2 units exist between the chains (Figure 2a). In addition, the distances of H−H in H_2 units are 0.764 and 0.779 Å, while the nearest In−In distance is 2.501 Å. For the P-1 structure, illustrated in Figure 2b, In atoms can be viewed as being composed of a slightly distorted body-centered tetragonal (bct) lattice, while seen from the b-axis, H_2 and slightly distorted H_3 units alternately pack. For H_2 units, the H−H length is 0.841 Å, while for H_3 units, there exist two different types, and the H−H distances are 0.846, 0.875 Å and 0.847, 0.876 Å, respectively. The shortest In−In length is 3.587 Å. For

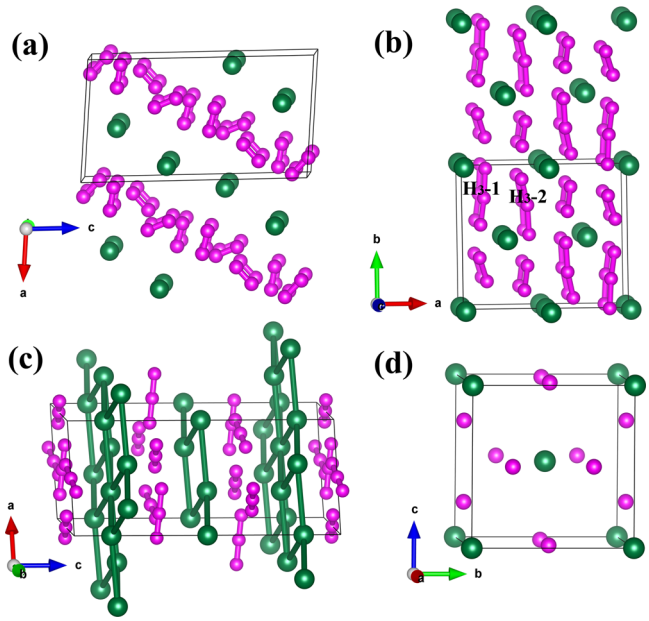

Figure 2. Crystal structures of InH_5-$P2_1/m$, InH_5-P-1, InH_3-R-3, and AlH_3-Pm-3m. Green atoms depict In, while pink atoms represent H. (a) InH_5-$P2_1/m$ at 200 GPa, (b) InH_5-P-1 at 300 GPa, (c) InH_3-R-3 at 200 GPa, and (d) AlH_3-Pm-3m at 200 GPa.

DOI: 10.1021/acs.inorgchem.5b01684
Inorg. Chem. 2015, 54, 9924−9928

InH_3 stoichiometry, it adopts *R*-3 symmetry at 200 GPa (Figure 2c), in which In atoms form a network with a coordination number of 6, while H atoms make up linear H_3 units. In addition, in H_3 units the nearest H−H bonding distance is 0.872 Å, and the close In−In distance is 2.545 Å. However, AlH_3 is a sister of InH_3 with *Pm*-3*n* symmetry,[39] where the metal atoms make up bcc and H is present in atomic form (Figure 2d). The corresponding structural information for InH_3 and InH_5 at selected pressures is listed in Table S1. The bonding nature will be discussed in the following. It is necessary to judge whether a phase is stable or not in lattice dynamics. Figure 3 depicts the calculated phonon dispersions and

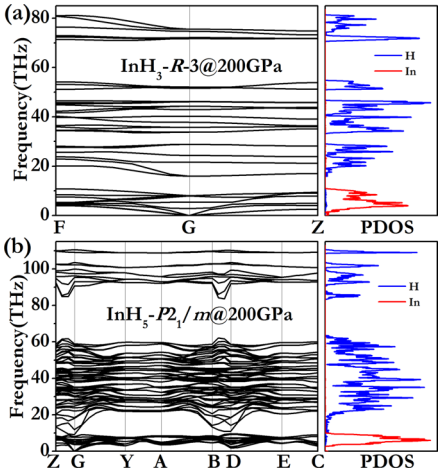

Figure 3. Phonon band structure and projected phonon DOS charts for (a) InH_3-*R*-3 and (b) InH_5-$P2_1/m$ at 200 GPa, respectively.

projected density of states (PHDOS) for InH_3-*R*-3 and InH_5-$P2_1/m$ at different pressures. The analysis reveals that there is no imaginary phonon mode throughout the Brillouin zone, indicating the dynamical stability of the above phases. Moreover, from visualization of the phonon modes, two distinct frequency branches can be observed. The low-frequency region (<10 THz) comes mainly from the vibrations of In atoms, and the high end of the modes corresponds to H atoms, due to the higher atomic mass of In than H.

Pressure-induced metalization and the corresponding electronic properties motivate us to investigate the electronic band structures and density of states (DOS) of InH_3-*R*-3 and InH_5-$P2_1/m$ at selected pressures, as graphed in Figure 4. Electronic band structures show that these two structures exhibit a metallic feature with several bands crossing the Fermi level. From the DOS, we see that there exists strong hybridization between H_s, In_s, and In_p around the Fermi level. Subsequently, to gain more insight into the bonding nature between the atoms, the electron localization functions (ELF) calculations were performed for InH_3-*R*-3 and InH_5-$P2_1/m$ at 200 GPa, respectively, as shown in Figure 5a and b. On the basis of the structural feature of higher pressure phase InH_5-*P*-1, we also calculated its ELF (Figure 5c). For InH_3-*R*-3, we selected a 2D map containing only linear-type H_3 units (Figure 5a). The ELF value of coplanar linear-type H_3 units is more than 0.9, illustrating the formation of covalent bonds, as expected from the H−H distance of 0.872 Å. For the InH_5-$P2_1/m$ phase, as shown in Figure 5b, the H_2 units are also characterized by a covalent bond with the electron localizing around them, while for the higher pressure phase InH_5-*P*-1, the

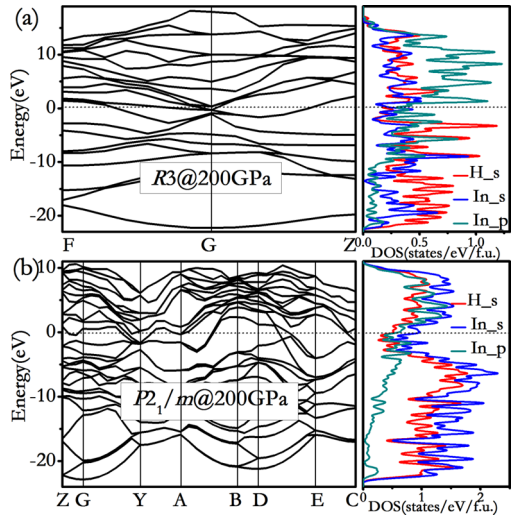

Figure 4. Calculated electronic band structure and partial density of states (PDOS) for (a) InH_3-*R*-3 and (b) InH_5-$P2_1/m$ at 200 GPa, respectively.

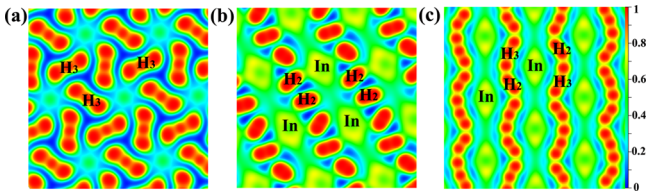

Figure 5. Electron localization function (ELF) maps of (a) InH_3-*R*-3 (200 GPa), (b) InH_5-$P2_1/m$ (200 GPa), and (c) InH_5-*P*-1 (300 GPa), respectively.

ELF value is higher than 0.9, suggesting strong polar covalent bonds form between the nonlinear-type H_3 units and H_2 units (Figure 5c). For the three structures, the ELF value is smaller than 0.5 between In and H atoms, which illustrates that the formation of In−H covalent bonds is impossible. The charge distributions for each element in InH_3-*R*-3, InH_5-$P2_1/m$, and InH_5-*P*-1 structures at different pressures were given by the Bader charge analysis, as displayed in Table S2. It shows that there exists ionic bonding between the In and H atoms with the charges transferring from In to H atoms. As the electronegativity value (1.78) of In is smaller than H (2.2), charges transfer from In to H. When the additional charges transfer to H atoms, material energy is decreased by forming H−H covalent bonds. This might be the physical mechanism to form "H_2/H_3" units in the InH_3 and InH_5 compounds, and many theoretical studies have reported that H_2 and H_3 units have been found in some hydrides.[16,17,40] In addition, we analyzed the pressure dependence of the H−H distance in H_3 units, as shown in Figure S1. It shows the general trend of the H−H distance decreasing with increasing pressure in both InH_3-*R*-3 and InH_5-*P*-1 structures. Moreover, the difference between the *z* and *d* distances in a $H^-\cdots H_2$ fragment vs their sum for H_3 units in InH_5 at different pressures was also calculated (Figure S2). We note that the value of $z-d$ gradually goes to zero as the pressure is increased (Figure S2), which indicates that pressure makes the H_3 units more stable.

Because the high-pressure phases of InH_3-*R*-3 and InH_5-$P2_1/m$ are metallic, they may be high-temperature superconductors. Hence, we further explored the superconductivities for InH_3-*R*-3 and InH_5-$P2_1/m$ at different pressures by calculating the

DOI: 10.1021/acs.inorgchem.5b01684
Inorg. Chem. 2015, 54, 9924−9928

electron−phonon coupling (EPC) parameter λ, the logarithmic average phonon frequency ω_{log}, and the Eliashberg phonon spectral function $\alpha^2F(\omega)$. For InH_3-*R*-3 and InH_5-$P2_1/m$ at 200 and 150 GPa, the obtained EPC parameters λ are 0.92 and 0.85 and the calculated ω_{log} are 666.8 and 509 K, respectively. The estimated T_c values reach 34.1−40.5 K (InH_3-*R*-3) and 22.4−27.1 K (InH_5-$P2_1/m$) considering the Coulomb pseudopotential μ^* of 0.1 and 0.13. Owing to the fact that the λ of InH_3-*R*-3 is relatively higher than that of InH_5-$P2_1/m$, the InH_3-*R*-3 structure has a quite strong EPC. We calculated the superconducting critical temperature T_c for InH_3-*R*-3 as a function of pressure. The values of λ, ω_{log}, and $N(E_f)$ at different pressures are summarized in Table 1. With increasing pressure, the calculated average frequency ω_{log} increases, but λ and $N(E_f)$ decrease. Hence, we think that the decrease of the T_c values with pressure may result from the diminishing λ and $N(E_f)$.

Table 1. Calculated Electron−Phonon Coupling Parameters, Electronic Density of States at the Fermi Level $N(E_f)$ (States/Spin/Ry/Unit Cell), Logarithmic Average Phonon Frequency ω_{log}, and Superconducting Critical Temperatures T_c for InH_3-*R*-3 at Different Pressures

P (GPa)	ω_{log} (K)	$N(\varepsilon_f)$	λ	T_c(K)μ^* = 0.1	T_c(K)μ^* = 0.13
200	666.829	7.589	0.919	40.499	34.090
250	729.191	6.837	0.857	39.085	32.270
300	740.273	6.364	0.837	37.972	31.133

Figure 6 presents the corresponding Eliashberg spectral function $\alpha^2F(\omega)$ and EPC integrated $\lambda(\omega)$ for InH_3-*R*-3 and InH_5-$P2_1/m$ at 200 and 150 GPa, respectively. For InH_3-*R*-3 and InH_5-$P2_1/m$, the In atoms contribute to the low frequency (<11 and 11.6 THz), which accounts for 46.4% and 46% of the total λ, while high-frequency vibrational modes of H provide a contribution of 53.6% and 54% in λ, respectively. The results indicate that In and H atoms contribute equally to T_c.

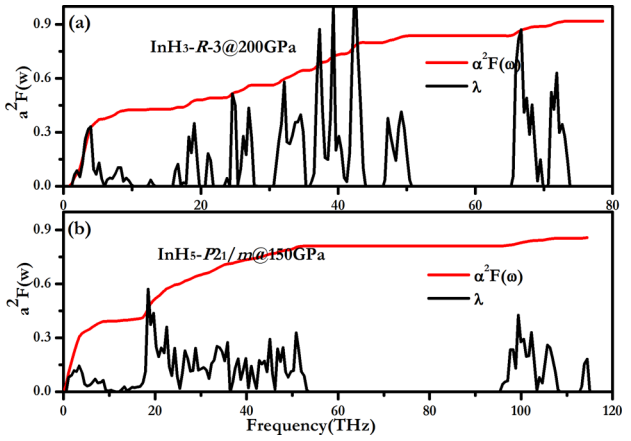

Figure 6. Eliashberg phonon spectral function $\alpha^2(\omega)$ and the partial electron−phonon integration $\lambda(\omega)$. (a) InH_3-*R*-3 at 200 GPa and (b) InH_5-$P2_1/m$ at 150 GPa.

CONCLUSION

To sum up, we searched for the high-pressure crystal structures of the In−H system by the evolutionary algorithm USPEX coupled with first-principles calculations at pressure up to 300 GPa. The stoichiometries InH_3 and InH_5 are found to be stable at high pressure. The phase of InH_5-$P2_1/m$ is stable in the pressure range of 120−223 GPa. Then InH_5 decomposes into InH_3 (*R*-3) and H_2 at 233 GPa, and InH_3 remains perfect up to 300 GPa. Interestingly, the hydrogenic sublattices are made up of H_2 or H_3 units in the stable phases. Further, by the application of the Allen−Dynes-modified McMillan equation, the predicted T_c values of *R*-3-InH_3 and $P2_1/m$-InH_5 are 34.1−40.5 K at 200 GPa and 22.4−27.1 K at 150 GPa. Our finding can hopefully encourage experiments to synthesize these proposed phases of indium hydrides at high pressure.

ASSOCIATED CONTENT

Supporting Information

The Supporting Information is available free of charge on the ACS Publications website at DOI: 10.1021/acs.inorgchem.5b01684.

Calculated structural parameters and Bader analysis for InH_3 and InH_5 at their corresponding pressures; the pressure dependence of the H−H distance in H_3 units in InH_3-*R*-3 and InH_5-*P*-1 structures; the difference between the *z* and *d* distances in an $H^-\cdots H_2$ fragment plotted vs their sum for H_3 units in InH_5 at different pressures (PDF)

AUTHOR INFORMATION

Corresponding Author

*E-mail: cuitian@jlu.edu.cn. Tel/Fax: +86-431-85168825.

Notes

The authors declare no competing financial interest.

ACKNOWLEDGMENTS

This work was supported by the National Basic Research Program of China (No. 2011CB808200), National Natural Science Foundation of China (Nos. 51572108, 11204100, 11504127, 11574109, 11404134), Program for Changjiang Scholars and Innovative Research Team in University (No. IRT1132), National Fund for Fostering Talents of Basic Science (No. J1103202), China Postdoctoral Science Foundation (2012M511326, 2013T60314, and 2014M561279), Graduate Innovation Fund of Jilin University (2015102), and EFree, an Energy Frontier Research Center funded by the DOE, Office of Science, Basic Energy Sciences, under Award No. DE-SC-0001057 (salary support for H.L.). The infrastructure and facilities used at Carnegie were supported by NNSA Grant No. DE-NA-00006, CDAC. Parts of calculations were performed at the High Performance Computing Center (HPCC) of Jilin University,

REFERENCES

(1) Ashcroft, N. W. *Phys. Rev. Lett.* **1968**, *21*, 1748−1749.
(2) Zha, C.-S.; Liu, Z.; Hemley, R. J. *Phys. Rev. Lett.* **2012**, *108*, 146402.
(3) Feng, J.; Grochala, W.; Jaroń, T.; Hoffmann, R.; Bergara, A.; Ashcroft, N. W. *Phys. Rev. Lett.* **2006**, *96*, 017006.
(4) Pickard, C. J.; Needs, R. J. *Phys. Rev. Lett.* **2006**, *97*, 045504.
(5) Yao, Y.; Tse, J. S.; Ma, Y.; Tanaka, K. *Europhysics Letters (EPL)* **2007**, *78*, 37003.
(6) Chen, X. J.; Struzhkin, V. V.; Song, Y.; Goncharov, A. F.; Ahart, M.; Liu, Z.; Mao, H. K.; Hemley, R. J. *Proc. Natl. Acad. Sci. U. S. A.* **2008**, *105*, 20−3.
(7) Eremets, M. I.; Trojan, I. A.; Medvedev, S. A.; Tse, J. S.; Yao, Y. *Science* **2008**, *319*, 1506−9.

DOI: 10.1021/acs.inorgchem.5b01684
Inorg. Chem. 2015, 54, 9924−9928

(8) Chen, X.-J.; Wang, J.-L.; Struzhkin, V. V.; Mao, H.-k.; Hemley, R. J.; Lin, H.-Q. *Phys. Rev. Lett.* **2008**, *101*10.1103/PhysRevLett.101.077002.
(9) Martinez-Canales, M.; Oganov, A. R.; Ma, Y.; Yan, Y.; Lyakhov, A. O.; Bergara, A. *Phys. Rev. Lett.* **2009**, *102*10.1103/PhysRevLett.102.087005.
(10) Kim, D. Y.; Scheicher, R. H.; Ahuja, R. *Phys. Rev. Lett.* **2009**, *103*, 077002.
(11) Zhou, D.; Jin, X.; Meng, X.; Bao, G.; Ma, Y.; Liu, B.; Cui, T. *Phys. Rev. B: Condens. Matter Mater. Phys.* **2012**, *86*, 014118.
(12) Duan, D.; Liu, Y.; Tian, F.; Li, D.; Huang, X.; Zhao, Z.; Yu, H.; Liu, B.; Tian, W.; Cui, T. *Sci. Rep.* **2014**, *4*, 6968.
(13) Liu, Y.; Duan, D.; Tian, F.; Li, D.; Sha, X.; Zhao, Z.; Zhang H.; Wu G.; Yu H.; Liu B.; Cui, T. arXiv preprint arXiv:1503.08587, **2015**.
(14) Ma, Y.; Duan, D.; Li, D.; Liu, Y.; Tian, F.; Huang, X.; Zhao Z.; Yu Y.; Liu B.; Cui, T. arXiv preprint arXiv:1506.03889, **2015**.
(15) Baettig, P.; Zurek, E. *Phys. Rev. Lett.* **2011**, *106*, 237002.
(16) Hooper, J.; Zurek, E. *Chem. - Eur. J.* **2012**, *18*, 5013−21.
(17) Shamp, A.; Hooper, J.; Zurek, E. *Inorg. Chem.* **2012**, *51*, 9333−42.
(18) Ye, X.; Hoffmann, R.; Ashcroft, N. W. *J. Phys. Chem. C* **2015**, *119*, 5614−5625.
(19) Li, Y.; Hao, J.; Liu, H.; Tse, J. S.; Wang, Y.; Ma, Y. *Sci. Rep.* **2015**, *5*, 9948.
(20) Liu, Y.; Duan, D.; Tian, F.; Li, D.; Sha, X.; Wang, C.; Zhang, H.; Yang, T.; Liu, B.; Cui, T. *J. Phys. Chem. C* **2015**, *119*, 15905−15911.
(21) Hu, C.-H.; Oganov, A. R.; Zhu, Q.; Qian, G.-R.; Frapper, G.; Lyakhov, A. O.; Zhou, H.-Y. *Phys. Rev. Lett.* **2013**, *110*, 165504.
(22) Graetz, J.; Reilly, J. J.; Yartys, V. A.; Maehlen, J. P.; Bulychev, B. M.; Antonov, V. E.; Tarasov, B. P.; Gabis, I. E. *J. Alloys Compd.* **2011**, *509*, S517−S528.
(23) Gao, G.; Wang, H.; Bergara, A.; Li, Y.; Liu, G.; Ma, Y. *Phys. Rev. B: Condens. Matter Mater. Phys.* **2011**, *84*, 064118.
(24) Hunt, P.; Schwerdtfeger, P. *Inorg. Chem.* **1996**, *35*, 2085−2088.
(25) Oganov, A. R.; Glass, C. W. *J. Chem. Phys.* **2006**, *124*, 244704.
(26) Oganov, A. R.; Lyakhov, A. O.; Valle, M. *Acc. Chem. Res.* **2011**, *44*, 227−237.
(27) Lyakhov, A. O.; Oganov, A. R.; Stokes, H. T.; Zhu, Q. *Comput. Phys. Commun.* **2013**, *184*, 1172−1182.
(28) Perdew, J. P.; Burke, K.; Ernzerhof, M. *Phys. Rev. Lett.* **1996**, *77*, 3865.
(29) Kresse, G.; Furthmüller, J. *Comput. Mater. Sci.* **1996**, *6*, 15−50.
(30) Kresse, G.; Joubert, D. *Phys. Rev. B: Condens. Matter Mater. Phys.* **1999**, *59*, 1758.
(31) Parlinski, K.; Li, Z.; Kawazoe, Y. *Phys. Rev. Lett.* **1997**, *78*, 4063.
(32) Togo, A.; Oba, F.; Tanaka, I. *Phys. Rev. B: Condens. Matter Mater. Phys.* **2008**, *78*, 134106.
(33) Bader, R. F. *Acc. Chem. Res.* **1985**, *18*, 9−15.
(34) Henkelman, G.; Arnaldsson, A.; Jónsson, H. *Comput. Mater. Sci.* **2006**, *36*, 354−360.
(35) Tang, W.; Sanville, E.; Henkelman, G. *J. Phys.: Condens. Matter* **2009**, *21*, 084204.
(36) Giannozzi, P.; Baroni, S.; Bonini, N.; Calandra, M.; Car, R.; Cavazzoni, C.; Ceresoli, D.; Chiarotti, G. L.; Cococcioni, M.; Dabo, I.; Dal Corso, A.; de Gironcoli, S.; Fabris, S.; Fratesi, G.; Gebauer, R.; Gerstmann, U.; Gougoussis, C.; Kokalj, A.; Lazzeri, M.; Martin-Samos, L.; Marzari, N.; Mauri, F.; Mazzarello, R.; Paolini, S.; Pasquarello, A.; Paulatto, L.; Sbraccia, C.; Scandolo, S.; Sclauzero, G.; Seitsonen, A. P.; Smogunov, A.; Umari, P.; Wentzcovitch, R. M. *J. Phys.: Condens. Matter* **2009**, *21*, 395502.
(37) Allen, P. B.; Dynes, R. C. *Phys. Rev. B* **1975**, *12*, 905−922.
(38) Pickard, C. J.; Needs, R. J. *Nat. Phys.* **2007**, *3*, 473−476.
(39) Goncharenko, I.; Eremets, M. I.; Hanfland, M.; Tse, J. S.; Amboage, M.; Yao, Y.; Trojan, I. A. *Phys. Rev. Lett.* **2008**, *100*, 045504.
(40) Hooper, J.; Zurek, E. *J. Phys. Chem. C* **2012**, *116*, 13322−13328.

DOI: 10.1021/acs.inorgchem.5b01684
Inorg. Chem. 2015, 54, 9924−9928